Ann. Geophys., 28, 1249–1261, 2010
www.ann-geophys.net/28/1249/2010/
doi:10.5194/angeo-28-1249-2010

Annales Geophysicae

On the correlation between Broad-Band ELF wave power and ion fluxes in the cusp

K. S. Jacobsen and J. I. Moen

Department of Physics, University of Oslo, Oslo, Norway

Received: 22 January 2010 – Revised: 10 May 2010 – Accepted: 1 June 2010 – Published: 9 June 2010

Abstract. We present a study of Broad-Band Extremely Low Frequency (BB-ELF) electric fields in the mid-altitude (4–6 Earth radii) cusp during periods of southward interplanetary magnetic field, using data from the Cluster spacecraft. Magnetospheric boundary layers are identified and classified according to particle precipitation characteristics. We find that the BB-ELF is contained within the cusp ion precipitation region, and its onset is closely co-located with the equatorward edge of the cusp ion dispersion signature. Previous studies have shown a positive correlation between BB-ELF and downward ion number flux. In this study, we compare the correlation coefficients of BB-ELF wave power versus the ion number and energy fluxes for upward, downward and total field-aligned fluxes. There is a greater degree of correlation between the total field-aligned flux and wave power than between the downward flux and wave power, which indicates that the BB-ELF wave generation is independent of ion beam direction. Our results support the idea of a local ion – BB-ELF wave interaction.

Keywords. Magnetospheric physics (Energetic particles, precipitating) – Space plasma physics (Wave-particle interactions)

1 Introduction

A commonly occurring feature in the precipitation regions near the open-closed field line boundary (OCB) is intense low-frequency fluctuations of the electric field. It has been observed at altitudes ranging from the ionosphere up to 10 Earth radii (e.g. Gurnett and Frank, 1977; Maynard et al., 1982; Sugiura et al., 1982; Gurnett et al., 1984; Marklund et al., 1990; Matsuoka et al., 1991, 1993; Kintner et al., 1996; Stasiewicz et al., 2000; Ivchenko and Marklund, 2001; Grison et al., 2005).

This kind of fluctuations is commonly referred to as broadband extremely low frequency (BB-ELF) electric fields (e.g. Wahlund et al., 1998; Knudsen et al., 1998; Kintner et al., 2000; Lund et al., 2000; Lynch et al., 2002; Hamrin et al., 2002; Bogdanova et al., 2004; Burchill et al., 2004; Backrud et al., 2005; Tam et al., 2005). The term BB-ELF has been used to refer to different frequency ranges by different authors, but generally it covers a frequency range from below the ion cyclotron frequency to above the ion plasma frequency.

Ivchenko and Marklund (2001) analyzed 6 months of electric and magnetic field measurements from the Astrid-2 microsatellite, whose orbit was at an altitude of 1000 km. They found that low frequency electromagnetic activity was persistently observed in the cusp region, but for periods of high geomagnetic activity also in the rest of the auroral oval. They suggested that the fluctuations were caused by the energy and plasma influx from the magnetosphere.

Miyake et al. (2003) surveyed the statistical properties of intense low-frequency electric field fluctuations at altitudes from 5000 to 10 000 km, using data from the Akebono (EXOS-D) satellite. They found that the fluctuations were most commonly observed in the prenoon cusp region, and noted that their dependence on the interplanetary magnetic field (IMF) and solar wind plasma parameters was similar to that of the ion outflow.

Golovchanskaya et al. (2006) statistically connected high-latitude electric and magnetic fluctuations to Birkeland field aligned currents, and noted that they occurred in an oval similar to the auroral oval and that they were insensitive to the direction of the field aligned current.

Kasahara et al. (2001) analyzed data from from Akebono, which orbited in the altitude range of 270–10 000 km, and found broadband low-frequency noise in the auroral region to be closely correlated with transverse acceleration of ions

Correspondence to: K. S. Jacobsen
(k.s.jacobsen@fys.uio.no)

Published by Copernicus Publications on behalf of the European Geosciences Union.

(TAI). They found the broadband noise to occur in the auroral oval and the cusp, with the most intense noise located in the cusp region.

Using the SCIFER rocket, which was launched into the prenoon cleft and reached an altitude of 1400 km, Kintner et al. (1996) demonstrated that there are narrow regions of TAI closely correlated with broadband low frequency electric fields and reduced density.

Matsuoka et al. (1993) investigated the relation between electric field fluctuations and particle precipitation in the cusp, using data from Akebono in the altitude range of 6000–10 000 km. They found a positive correlation with the precipitating ion flux. The correlation was best, and the fluctuation most intense, for southward IMF. They identified the fluctuations as Alfvén waves with a downward Poynting flux, and since they did not find a specific frequency peak in the power spectral density (PSD) they concluded that the waves are possibly generated in association with the plasma injection at the magnetopause.

Wahlund et al. (1998) analyzed data from two orbits of the Freja spacecraft, which had an apogee of 1750 km. They found the BB-ELF emissions to consist of several wave modes, and suggested a scenario where slow kinetic Alfvén waves cause intense transverse ion heating via BB-ELF emission.

Knudsen et al. (1998) found correlation between core ion energization, suprathermal electron bursts, and BB-ELF waves in the cusp, using data from the Freja spacecraft. In a similar study using data from Cluster at 4 R_E, Bogdanova et al. (2004) found correlation between suprathermal electron bursts, local ion heating, and BB-ELF waves.

Grison et al. (2005) and Sundkvist et al. (2005) investigated electromagnetic waves at frequencies near the proton cyclotron frequency in the cusp at 8–10 R_E altitude. Both found the waves to be Alfvén waves below the proton cyclotron frequency and Bernstein waves above, and presented evidence of local wave generation. Grison et al. (2005) suggested a coupling between the observed waves and ion heating.

The main objective of the present work is to reinvestigate the correlation between the ion flux and the BB-ELF wave power using Cluster data. Matsuoka et al. (1993) found BB-ELF to be correlated with the cusp ion and electron precipitation, but that the correlation coefficients varied from case to case, exceeding 0.5 in only half the cases. When investigating the correlation to BB-ELF, they considered the precipitating (downward) number flux. However, if the BB-ELF waves are generated locally by ion beams, as suggested by Grison et al. (2005) and Sundkvist et al. (2005), the beam direction should not matter.

Despite the availability of an increasing amount of high quality satellite data there has been made no further attempts to quantify the relationship between cusp ion fluxes and BB-ELF wave power after Matsuoka et al. (1993). In this study we will advance the work by Matsuoka et al. by considering both ion number and ion energy fluxes for upward, downward and total field-aligned fluxes. As mentioned above, the BB-ELF phenomenon has been roughly addressed to the auroral zone and is frequently associated with cusp ion precipitation. Here we make the first attempt to place the occurrence of BB-ELF waves in context of the open-closed boundary (OCB) and in relation to the equatorward and poleward edges of the cusp ion dispersion signature. We will demonstrate that the correlation between BB-ELF wave power and ion fluxes maximize when we treat cusp events individually.

The data analysis methods used are presented in Sect. 2. The results are presented in Sect. 3 and discussed in Sect. 4, followed by a brief summary in Sect. 5.

2 Data analysis

2.1 Data selection criteria

This study is based on data from the Cluster mission (Credland et al., 1997; Credland and Schmidt, 1997) between the years 2001 to 2005. The orbit of the Cluster spacecraft passes the mid-altitude (in this paper defined to be 4–6 Earth radii) cusp area in the autumn, so cusp passes in the months from July to November were investigated. This study focuses on crossings where the IMF was stable and oriented southward, (clock angles 135–225 degrees) in favor of magnetopause reconnection. Some crossings were eliminated due to lack of electric field data, IMF data or particle data. The final set of data comprises 59 cusp passes, 15 of which lack ion data and thus are useful only for comparing the onset of BB-ELF to the OCB. In order to compare the occurrence of BB-ELF to the cusp ion dispersion region, the ion spectra must be sufficiently clear to allow identification of its latitudinal span. For the correlation analysis, the data quality requirements were higher, and only data from 24 cusp passes cases were used.

Electric field data are provided by the Electric Fields and Waves (EFW) instrument (Gustafsson et al., 1997). Ion spectra are provided by the ion spectrometer (CIS) (Reme et al., 1997) and are used for identification of the cusp ion dispersion signature. Electron spectra are provided by the electron spectrometer (PEACE) (Johnstone et al., 1997) and are the primary means of OCB identification. The secondary means of OCB identification are high-energy electron measurements from the RAPID instrument (Wilken et al., 1997). Interplanetary magnetic field data are provided by the ACE satellite (Chiu et al., 1998; Smith et al., 1998). The timeshifted ACE data were obtained from the GSFC/SPDF OMNIWeb database.

2.2 Location of the BB-ELF region relative to the cusp ion dispersion region and the OCB

For each crossing the time at which the spacecraft crossed the OCB, and the start and end times of the ion dispersion

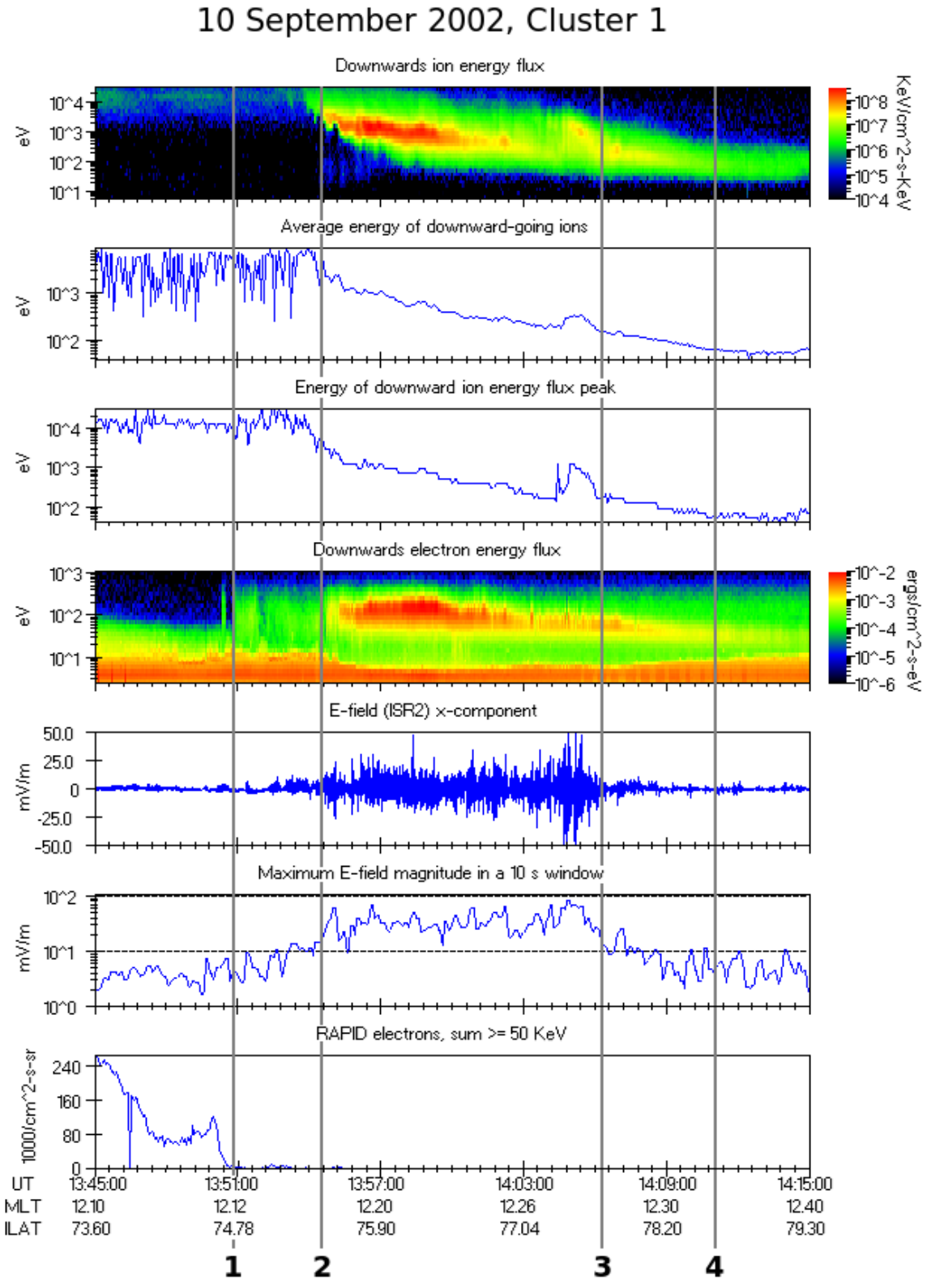

Fig. 1. An example of a cusp pass, with vertical lines marking the boundaries of interest. **1:** The open/closed boundary. Identified by the magnetosheath electron edge and by the drop in energetic electron flux. **2:** The start of the cusp ion dispersion, in this case coinciding with the onset of BB-ELF. **3:** The end of the BB-ELF region. **4:** The end of the cusp ion dispersion.

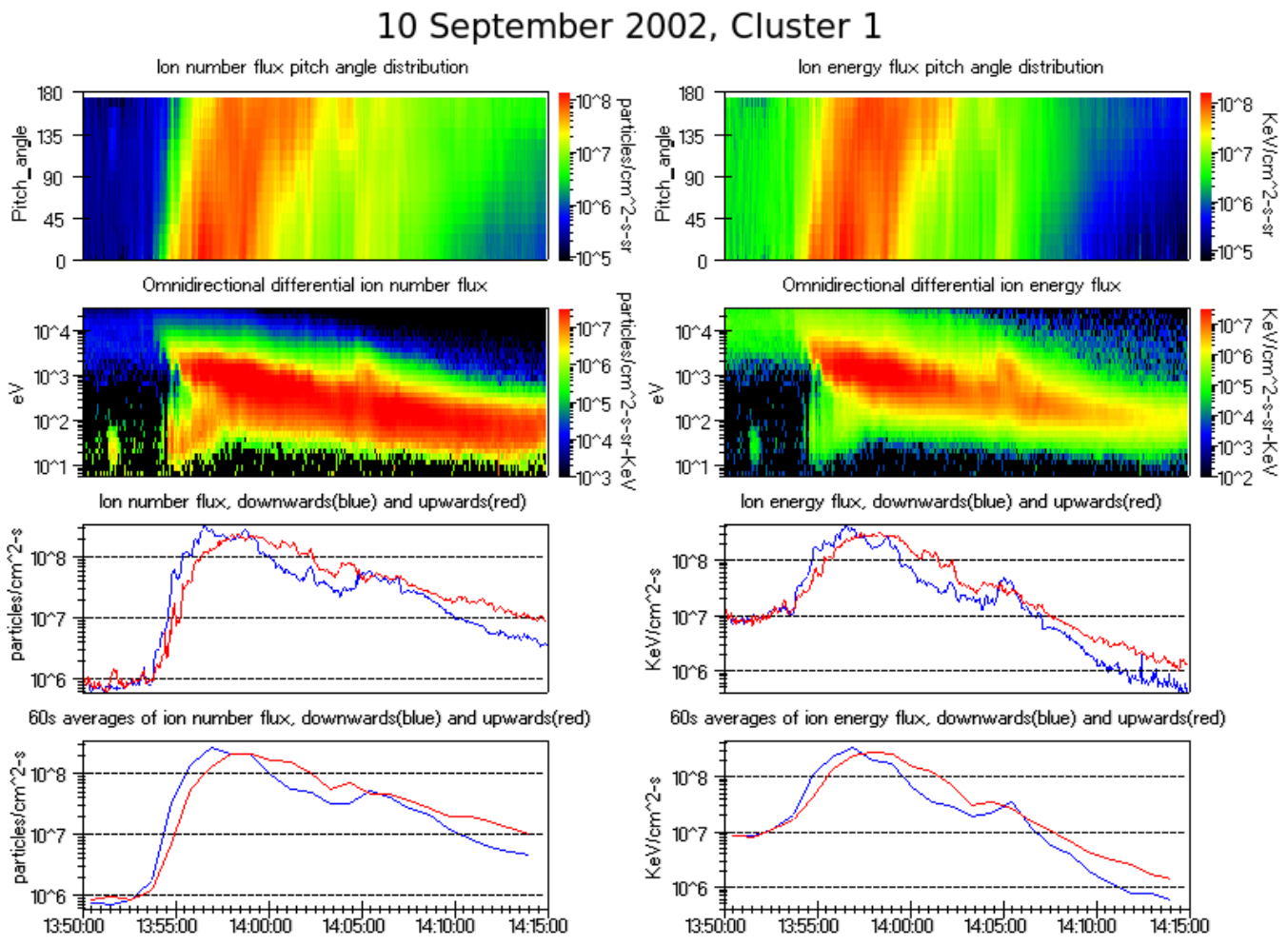

Fig. 2. Pitch angle distribution, omnidirectional flux, downward/upward fluxes and 60 s averaged downward/upward fluxes, for number flux in the left column and energy flux in the right column. For the data in this figure, a pitch angle of 0 is downwards and a pitch angle of 180 is upwards.

region and the BB-ELF region, are noted. The BB-ELF region is identified by rapid variations of the electric field with amplitudes significantly greater than the background. Amplitudes being consistently greater than 10 mV/m has been used as a guideline, but each case was manually inspected. Figure 1 shows an example of the times corresponding to the different boundary crossings used in this study. The OCB is identified by the electron edge as seen by PEACE and confirmed by the drop in the high-energy electron flux measured by RAPID (Lockwood, 1997; Onsager and Lockwood, 1997; Moen et al., 1996, 2004; Bogdanova et al., 2004).

The noted times are converted into the magnetic local time (MLT) and invariant latitude (ILAT) of the various observed boundaries, allowing comparison of the magnetic positions of the OCB, the BB-ELF region and the poleward and equatorward edges of the energy dispersed cusp ion injections.

2.3 Correlation between BB-ELF wave power and ion fluxes

To investigate the connection of the BB-ELF to particle fluxes, correlation coefficients (Pearson's r) were calculated for the BB-ELF wave power versus downward, upward and total field-aligned ion fluxes, considering both number and energy fluxes. Note that the total field-aligned flux is not the net flux, but a sum of the absolute upward and downward fluxes. More on this, as well as the details of the ion data sources and the flux calculations, is located in the appendix. Calculations were performed using a sliding window, in which the correlation coefficients between the average power of the electric field in the range 0.75 Hz–11 Hz and the average fluxes of ions were computed. The lower limit of the frequency range has been chosen to avoid any erroneous signals due to the spacecraft spin, which is roughly 0.25 Hz. When operating in normal mode, the electric field

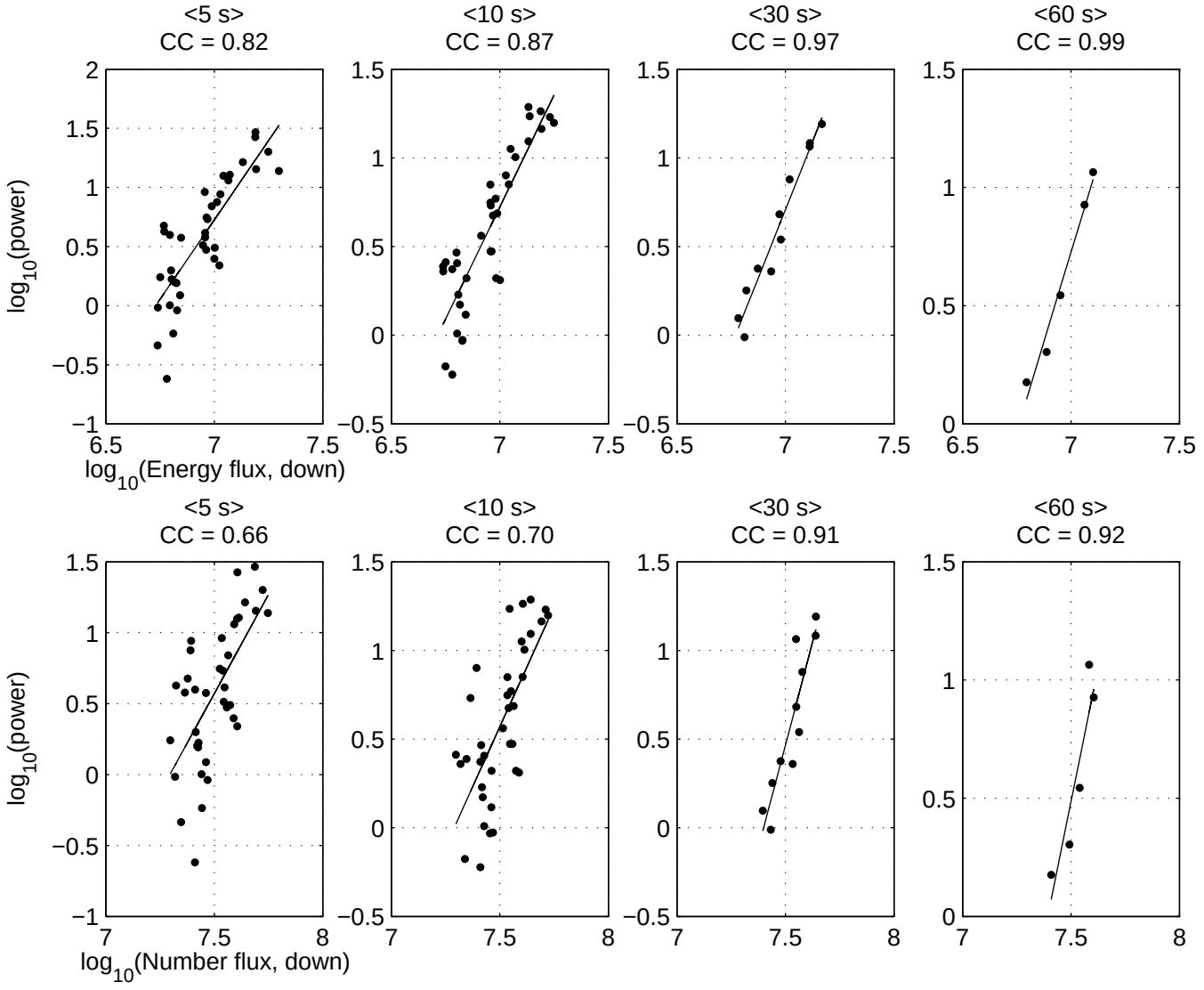

Fig. 3. Plots of BB-ELF wave power versus ion fluxes for the 6 September 2001 cusp pass by Cluster 4. The top row shows ion energy flux, the bottom ion number flux. The four columns show how the correlation varies with different time averaging. For each panel the x-axis is the logarithm of the average flux within the window and the y-axis is the logarithm of the average electric field power in the range 0.75–11 Hz within the window. The data is plotted as points, and the lines are linear fits. Above each panel is the correlation coefficient (CC) for the linear fit shown in that panel.

experiment on Cluster has a sampling rate of 25 Hz. The upper limit of the chosen frequency range is slightly below the resulting Nyquist frequency. Figure 2 shows an example of the pitch angle distribution of the number and energy fluxes, as well as the effect of a 60 s averaging of the downward and upward number and energy fluxes.

The CIS instrument is mounted on the side of the Cluster spacecraft, and thus requires at least one spin period to collect a full ion distribution (Reme et al., 1997). This sets a lower limit of 4 s on the sampling time of the ion data. Sometimes, several spins are required. If the calculations are performed at the measurement limit of the instrument, the correlation will not be good. Averaging over several samples yields better correlation coefficients. If viewed as a function of the window size (i.e. time averaging) the correlation rises sharply at first and then levels off, in those cases where there is a definite correlation to be found. The correlation coefficient plateau was reached for time averages between 20 and 60 s. See Fig. 3 for an example of this behavior.

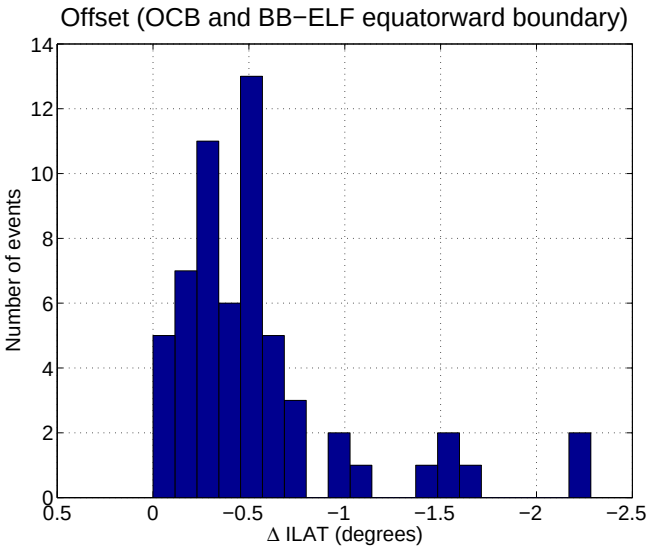

Fig. 4. Histogram of the latitudinal distance between the OCB and the onset of the BB-ELF activity. A negative value means the BB-ELF starts poleward of the OCB.

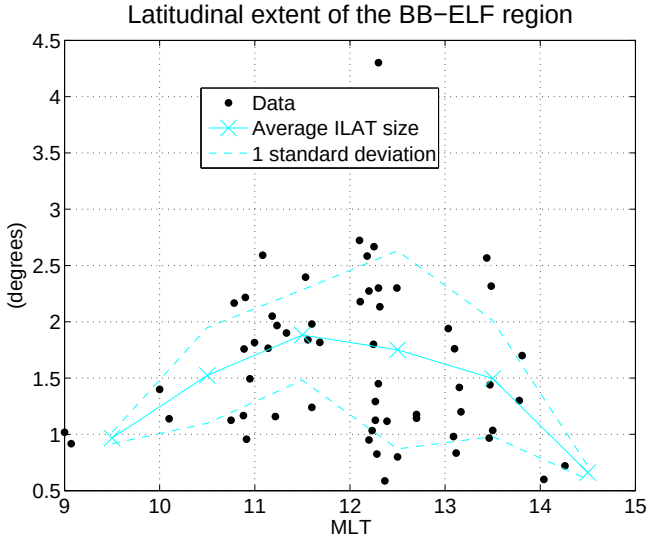

Fig. 5. The latitudinal extent of the BB-ELF region as a function of MLT. The solid line shows the average value for each 1-h bin, with ± one standard deviation shown by the dashed line. There is a clear tendency towards a broader region around noon, but with a large variation in latitudinal extent from case to case.

3 Results

3.1 Location of the BB-ELF region relative to the cusp ion dispersion region and the OCB

Figure 4 shows the latitudinal distance between the OCB and the equatorward boundary of the BB-ELF region. The latitudinal difference is mostly less than 1 degree.

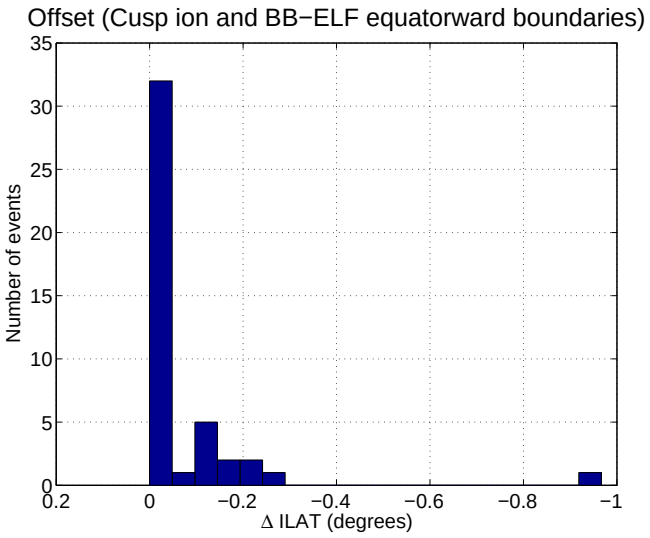

Fig. 6. Histogram of the latitudinal distance between the onset of the cusp ion dispersion and the onset of BB-ELF. A negative value means the BB-ELF start poleward of the onset of ion dispersion.

Figure 5 shows the latitudinal extent of the BB-ELF region as a function of the MLT at which the OCB is observed. The boundary crossings were almost along the magnetic meridian and hence the change in MLT during each pass was negligible. There is a large spread in the data points but the average value for the BB-ELF latitude span shows a clear maximum around noon.

Figure 6 shows the latitudinal distance between the boundaries corresponding to the onset of the ion dispersion and the onset of the BB-ELF. For most cases, they are co-located. In the other cases, the BB-ELF is always preceded by the ion dispersion. The offset in the latitude of these two boundaries is small, with a mean value of 0.06 degrees.

Figure 7 shows the latitudinal distance between the boundaries corresponding to the poleward end of the cusp ion dispersion signature and the poleward edge of the BB-ELF region. There is a greater spread in the offset of these two boundaries at the poleward end than was the case on the equatorward side, with a mean value of 1.5 degrees. However, the poleward edge of the ion dispersion signature is not so sharp and well defined as the equatorward ion edge. Notably, the ion dispersion signature always extends poleward of the BB-ELF region.

A byproduct of this study is a statistical measure of the width of the magnetosheath electron edge. In a statistical study of the electron edge, Bogdanova et al. (2006) found its latitudinal extent to vary between 0 and 2 degrees ILAT, with a median of 0.2 degrees. For the data in this study, it varies between 0 and 2.25 degrees ILAT, with a median of 0.38 degrees.

Table 1. Each row shows a summary of the correlation coefficients of the Power Spectral Density (PSD) of the electric field fluctuations around 1 Hz versus one type of ion flux, with each column containing the number of cases with a correlation within the interval shown in the column header. 30 s averages of the wave power and flux levels were used for the calculations. The total number of cases is 26. "field-aligned" flux is the sum of the absolute values of upward and downward flux. A summary of the correlation results of Matsuoka et al. (1993) have been included for comparison.

PSD vs.	Correlation, using 30 s averaging. # of cases.						
	< -0.8	-0.8 to -0.6	-0.6 to -0.4	None	0.4 to 0.6	0.6 to 0.8	>0.8
Energy flux, downwards	0	2	1	6	5	7	5
Energy flux, field-aligned	0	1	2	7	5	2	9
Number flux, downwards	0	0	2	5	6	5	8
Number flux, field-aligned	0	0	0	4	7	4	11
From Matsuoka, Fig. 10				11	7	9	3

3.2 Correlation between BB-ELF wave power and ion fluxes

For some cusp passes the cusp contained additional injection events. Treating these as one event will result in very poor correlation, so they must be carefully separated, if possible. Figure 8 shows the Cluster 1 10 September 2002 pass, in which particles coming from two injection events are seen. This pass has been split into two events, as indicated by the red boxes. When treated as one event, the correlation coefficient of the BB-ELF wave power versus the total field-aligned ion number flux, using 30 s averages, was 0.12. After splitting into two events, the correlation coefficients were 0.37 and 0.93, respectively.

Table 1 shows the number of cases with various sign and strength of the correlation between the BB-ELF wave power and the energy and number fluxes. The results of Matsuoka et al. (1993) have been included here for comparison. For this table 30 s averages were used for the calculations to facilitate comparison with Matsuoka et al., who used 28 s averages for their calculations. Table 2 shows the same as the previous table, but for 60 s averages. This ensures that the correlation has reached the plateau level for all cases. Upward fluxes were found to have similar or less correlation than the downward fluxes and are not shown. The field-aligned fluxes show higher degrees of correlation than the downward fluxes. To show this more clearly, the results shown in Table 2 were filtered using the Student's t-test. Only correlation coefficients with a significance level of 95% or greater were kept, and the correlation values greater than 0.6 were sorted using smaller correlation coefficient bins. The result of this is shown in Table 3.

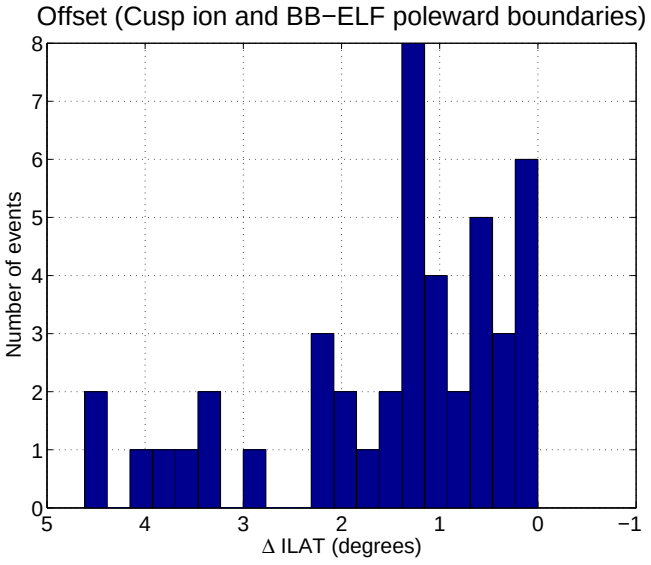

Fig. 7. Histogram of the latitudinal distance between the poleward end of the cusp ion dispersion and the poleward end of the BB-ELF region. A positive value means the ion dispersion extends poleward of the BB-ELF region.

4 Discussion

Ivchenko and Marklund (2001) used 6 months of data from the Astrid-2 microsatellite to study low frequency electric and magnetic field fluctuations in the high-latitude ionosphere at 1000 km altitude. They found that this phenomenon had a high occurrence rate in the dayside cusp/cleft region, but was also found in the nightside auroral oval. Miyake et al. (2003) used data from Akebono at an altitude of 5000 to 10 000 km to study low-frequency electric field fluctuations around the dayside cusp/cleft region. They found that the phenomenon occurred at lower altitudes for negative B_z than for positive B_z, and noted that it was associated with the cusp. The occurrence of broadband electric field fluctuations in the auroral oval and the cusp has also been noted by Golovchanskaya et al. (2006) and Kasahara et al. (2001). However, none of these studies investigated the exact positioning of the fluctuations in regards to the cusp, as their main focus was on other issues.

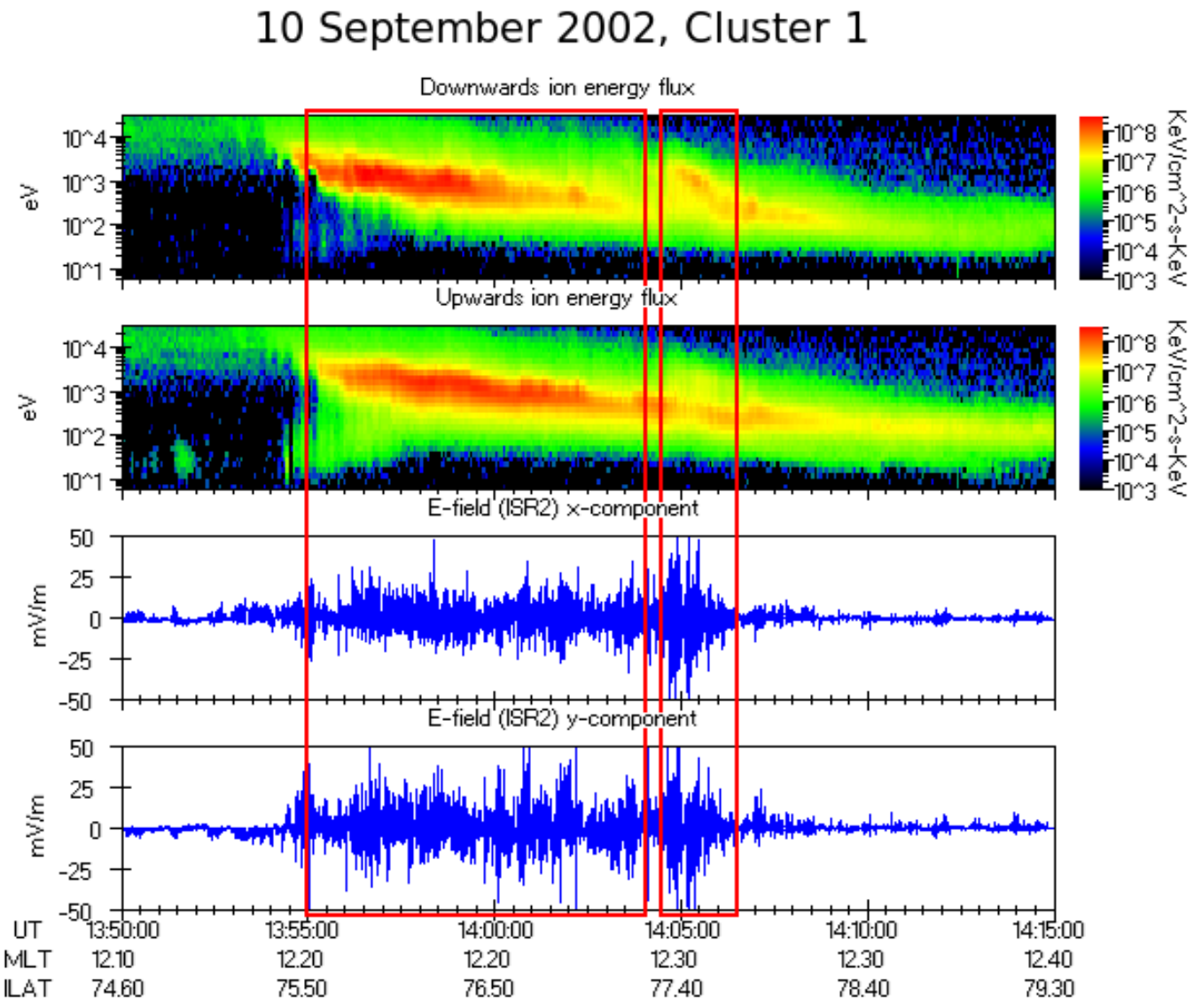

Fig. 8. The cusp pass of 10 September 2002. In the downward ion flux, two distinct injection events are clearly visible. The time intervals used when studying the correlation between BB-ELF power and ion flux are marked with red boxes. Note that these do not correspond exactly to the BB-ELF region defined in Fig. 1. The first box starts 30 s later than the onset of BB-ELF as shown in that figure, and there is a 30 s gap between the first and second box. This was done to avoid the transition areas.

In this study a detailed account of the location of the BB-ELF region with regard to the OCB and the cusp ion injection region has been presented. The BB-ELF region is contained within the cusp ion dispersion region, and was always present for the cases examined. The equatorward edge of the fluctuations corresponds closely to the equatorward edge of the cusp ion dispersion region, while the poleward edge of the fluctuations may deviate from the poleward edge of the cusp ion dispersion region by several degrees.

Electrons of magnetosheath origin will arrive in the ionosphere almost immediately after reconnection and hence represents the most accurate observable proxy of the OCB and is often referred to as the "low energy electron edge" of the LLBL (e.g. Lockwood, 1997; Topliss et al., 2001; Sandholt et al., 2002; Moen et al., 2004; Bogdanova et al., 2006). When no electron spectra are available, ion spectra may be used instead. As the onset of BB-ELF correspond closely to the onset of ion dispersion, it may serve as a proxy for the OCB such as the equatorward ion edge does. For this purpose, its accuracy would be about the same as the accuracy of the ion spectra, which have a maximum discrepancy of up to 2 degrees around magnetic noon.

The correlation between BB-ELF power and ion fluxes has been studied. Different frequencies of the BB-ELF are linked by power laws, as seen in Fig. 9. The break seen in the graph is a common signature of spectra in the cusp, and this kind

Table 2. Each row shows a summary of the correlation coefficients of the Power Spectral Density (PSD) of the electric field fluctuations around 1 Hz versus one type of ion flux, with each column containing the number of cases with a correlation within the interval shown in the column header. 60 s averages of the wave power and flux levels were used for the calculations. The total number of cases is 26. "field-aligned" flux is the sum of the absolute values of upward and downward flux.

PSD vs.	Correlation, using 60 s averaging. # of cases.						
	< -0.8	-0.8 to -0.6	-0.6 to -0.4	None	0.4 to 0.6	0.6 to 0.8	>0.8
Energy flux, downwards	2	1	0	4	5	4	10
Energy flux, field-aligned	1	1	1	5	3	4	11
Number flux, downwards	0	1	1	4	2	8	10
Number flux, field-aligned	0	0	1	2	3	6	14

Table 3. Each row shows a summary of the correlation coefficients of the Power Spectral Density (PSD) of the electric field fluctuations around 1 Hz versus one type of ion flux, with each column containing the number of cases with a correlation within the interval shown in the column header. 60 s averages of the wave power and flux levels were used for the calculations. Only correlation coefficients with a significance level of 95% or greater are included in this table. "field-aligned" flux is the sum of the absolute values of upward and downward flux.

PSD vs.	Correlation with significance $\geq$95% using 60 s averaging. # of cases.			
	0.6 to 0.7	0.7 to 0.8	0.8 to 0.9	>0.9
Energy flux, downwards	2	0	6	2
Energy flux, field-aligned	3	1	5	5
Number flux, downwards	5	2	5	4
Number flux, field-aligned	4	1	4	7

of double slope behavior is common in turbulent plasmas in general (e.g. Markovskii et al., 2008; Schekochihin et al., 2009; Shaikh and Zank, 2009 and the references therein). It signifies a different set of processes taking place at the different frequency ranges, the details of which are outside the scope of this study. The break occurs in the vicinity of the ion gyrofrequency, which changes with altitude. Nykyri et al. (2006) found that turbulent magnetic fields in the cusp were correlated with the field-aligned ion flux, and had a break in the power spectrum in the vicinity of the local ion cyclotron frequency. They showed that the break could be caused by damping of kinetic Alfvén waves and ion cyclotron waves.

The cusp may contain several injection events (Escoubet et al., 2008). The relation between ion fluxes and BB-ELF power may be different for each of these, and so they must be separated for a successful analysis. An example of this is shown in Fig. 8. This underscores the direct relationship between localized ion injection events and the BB-ELF phenomenon.

Whereas Matsuoka et al. (1993) only considered the downward number flux when investigating the connection between particles and BB-ELF, in this study both number and energy fluxes have been considered, for upward, downward and total field-aligned fluxes. In Table 1 the results of Matsuoka et al. have been included for comparison. Our results for the correlation between the downward ion number flux and

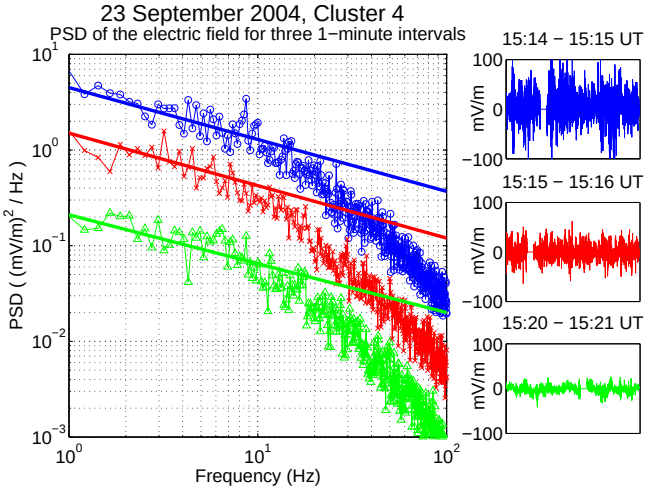

Fig. 9. Power spectral density (PSD) of the electric field observed by Cluster 4 during the 23 September 2004 cusp pass. Three one-minute intervals have been selected to show how the PSD graph changes for different fluctuation intensities. The electric field data are shown in the small panels on the right. The corresponding PSDs are shown with the same color in the main panel. At this time, the local proton gyrofrequency was 8.3 Hz. There is a break in the PSD in the vicinity of the proton gyrofrequency. Thick lines have been added as a visual aid to emphasize the break in the graph.

the BB-ELF wave power are similar to those of Matsuoka et al., but with a somewhat greater correlation. This may be a result of better instrumentation, or possibly a better selection of events. The fact that Matsuoka et al. did not include ions with energies lower than 500 eV in their calculations may also have influenced their results, as there is a noticeable flux of ions down to at least 200 eV (see for example Fig. 8). It is also possible that some of their events included injection events in addition to the normal cusp dispersion. It is clear that the total field-aligned fluxes show a greater degree of correlation with the BB-ELF wave power than the downward fluxes. Table 2 shows the same as Table 1, but using longer time averages for the calculations to ensure that we do not notice any effects of limited instrument time resolution. For all types of flux the correlation with the BB-ELF wave power exceeded 0.6 in more than half the cases, and 0.8 in more than a third. The field-aligned fluxes showed a greater degree of correlation with the BB-ELF wave power than the downward fluxes. This is seen most clearly in Table 3, where the results with a high positive correlation have been sorted in smaller bins, and only correlation values with a high significance have been included. These results support a different interpretation than the one suggested by Matsuoka et al.. They concluded that the waves are possibly generated in association with the plasma injection at the magnetopause, while the correlation with the total field-aligned ion fluxes found here suggests a local exchange of energy between ions and the BB-ELF waves. For a local generation of BB-ELF waves by ion beams, there should be no reason to have a distinction between upward and downward flux.

Correlation between BB-ELF waves and ion heating in the cusp has been reported by several authors (Knudsen et al., 1998; Bogdanova et al., 2004). The nature of the waves has been further investigated by Grison et al. (2005) and Sundkvist et al. (2005), who found evidence of local wave generation, with protons being a probable source of energy. They have shown that that while the wave activity below the proton gyrofrequency consists of Alfven waves, there are other wave modes dominating above the proton gyrofrequency. Matsuoka et al. (1993) dismissed local generation of the BB-ELF waves because they found no specific frequency peak in the PSD. However, they only covered the range 0.5 to 5 Hz, while the proton gyrofrequency at the altitude where their measurements were taken would be on the order of 100 Hz. The electric field instrument of Akebono had a sampling rate of 32 Hz, and thus would not be able to detect these effects. Matsuoka et al. found the Poynting flux to be directed downwards. In the results of Sundkvist et al., the Poynting flux of waves below the ion gyrofrequency was indeed found to be directed downwards, but at frequencies above the ion gyrofrequency it was directed upwards. As the proton gyrofrequency decreases with increasing altitude, this is a strong indication that waves are being generated locally. A full investigation of the nature of the waves comprising BB-ELF is outside the scope of this study. For more information on this topic, see the papers by Grison et al. (2005) and Sundkvist et al. (2005) and the references therein.

5 Summary

Electric field fluctuations (BB-ELF) in the cusp have been investigated, using five years of Cluster data. We have revisited the issue of correlation between BB-ELF and ion fluxes, which has previously been investigated by Matsuoka et al. (1993). We have also examined the location of BB-ELF relative to the OCB and the cusp ion dispersion boundaries. The main results are:

- The BB-ELF region was found to be contained within the cusp ion dispersion region.
- The equatorward boundary of the BB-ELF region was found to be co-located with the equatorward boundary of the cusp ion dispersion region.
- The BB-ELF wave power shows a strong correlation to ion fluxes.
- The BB-ELF wave power was found to have a greater degree of correlation with the total field-aligned fluxes than with the downward fluxes. This is an improvement over previous results, which only considered the downward ion number flux. Our results are consistent with the idea of a local ion – BB-ELF wave interaction.

Appendix A

Details of the ion data sources and the flux calculations

The ion data in this study has been gathered from the Cluster Active Archive database. The Cluster ion experiment consists of two parts; the Hot Ion Analyzer (HIA) and the Composition and Distribution Function analyzer (CODIF). For cusp studies, the CIS team recommends high sensitivity (HS), magnetospheric mode (MAG) data from HIA. If this is not available, magnetospheric mode CODIF data may be used. The ion experiment on Cluster 2 is not working, so for this spacecraft there is no ion data available. On Cluster 4, only the CODIF part of the ion experiment is working. Thus, for Cluster 1 and 3, the data products used were CP_CIS-HIA_HS_MAG_IONS_PF (differential ion number flux) and CP_CIS-HIA_HS_MAG_IONS_PEF (differential ion energy flux). For Cluster 4, the data products used were CP_CIS-CODIF_HS_H1_PF (differential ion number flux) and CP_CIS-CODIF_HS_H1_PEF (differential ion energy flux). All of these are level 3 data products. In MAG mode, the energy ranges of HIA and CODIF are 5 eV to 32 KeV and 25 eV to 40 KeV, respectively. The energy range of the instrument used by Matsuoka et al. (1993) was 13 eV

to 20 KeV. (Note, though, that Matsuoka et al. restricted their calculations to an ion energy range of 500 eV to 10 KeV.) The energy ranges of these instruments all cover the energy range of cusp ion precipitation, which mainly consists of ions with an energy between some hundred and some thousand eV. Both the HIA and CODIF files from the CAA have an angular resolution of 16 azimuth $\times$ 8 elevation angles ($22.5^\circ \times 22.5^\circ$), for a total of 128 solid angle bins.

The downward and upward fluxes are calculated as follows: First, a pitch angle is calculated for each bin of the CIS data, using magnetic field from the FGM instrument (Balogh et al., 1997). Then, the average downward differential flux for each energy bin is calculated as

$$\mathrm{DF}_{\mathrm{down}}(E) = \frac{\sum_{\theta=0}^{\frac{\pi}{2}} \mathrm{DF}(E,\theta)\cos(\theta)}{\text{Number Of Bins In The Sum}}$$

where DF is the differential flux and θ is the pitch angle. Similarly, the average upward differential flux for each energy bin is

$$\mathrm{DF}_{\mathrm{up}}(E) = -\frac{\sum_{\theta=\frac{\pi}{2}}^{\pi} \mathrm{DF}(E,\theta)\cos(\theta)}{\text{Number Of Bins In The Sum}}$$

This is summed over the energy range and multiplied by 2π (steradians of a half-sphere) to get the downward flux

$$F_{\mathrm{down}} = 2\pi \sum_{E_i} \mathrm{DF}_{\mathrm{down}}(E) dE$$

where E_i is the set of energy bins, and dE is the width of each energy bin. The upward flux is

$$F_{\mathrm{up}} = 2\pi \sum_{E_i} \mathrm{DF}_{\mathrm{up}}(E) dE$$

The total field-aligned flux is then defined as $F_{\mathrm{down}} + F_{\mathrm{up}}$. Note that as these are both positive numbers, this is not a net flux. We are concerned with the total amount of ions/energy passing through, not the net flux, as two equally strong counter-streaming ion populations should be able to excite more waves than a completely stagnant ion population even though they both have a net flux of zero. As a test, the correlation calculations were also performed using the absolute net flux. It was found to have a similar to or lesser correlation than the downward flux.

Acknowledgements. We acknowledge the CIS, PEACE, RAPID, EFW and FGM instrument teams and the ESA Cluster Active Archive for the use of Cluster data. We acknowledge the ACE instrument team for the use of ACE data. Timeshifted ACE data were obtained from the GSFC/SPDF OMNIWeb database at http://omniweb.gsfc.nasa.gov. We thank Philippe Escoubet for helpful discussions. This work has been supported by the Norwegian Research Council. We thank the reviewers for helpful comments.

Topical Editor R. Nakamura thanks two anonymous referees for their help in evaluating this paper.

References

Backrud, M., Tjulin, A., Vaivads, A., Andre, M., and Fazakerley, A.: Interferometric identification of ion acoustic broadband waves in the auroral region: CLUSTER observations, Geophys. Res. Lett., 32, L21109, doi:{10.1029/2005GL022640}, 2005.

Balogh, A., Dunlop, M., Cowley, S., Southwood, D., Thomlinson, J., Glassmeier, K., Musmann, G., Luhr, H., Buchert, S., Acuna, M., Fairfield, D., Slavin, J., Riedler, W., Schwingenschuh, K., and Kivelson, M.: The Cluster magnetic field investigation, Space Sci. Rev., 79, 65–91, 1997.

Bogdanova, Y., Fazakerley, A., Owen, C., Klecker, B., Cornilleau-Wehrlin, N., Grison, B., Andre, M., Cargill, P., Reme, H., Bosqued, J., Kistler, L., and Balogh, A.: Correlation between suprathermal electron bursts, broadband extremely low frequency waves, and local ion heating in the midaltitude cleft/low-latitude boundary layer observed by Cluster, J. Geophys. Res.-Space Phys., 109, A12226, doi:{10.1029/2004JA010554}, 2004.

Bogdanova, Y. V., Owen, C. J., Fazakerley, A. N., Klecker, B., and Rème, H.: Statistical study of the location and size of the electron edge of the Low-Latitude Boundary Layer as observed by Cluster at mid-altitudes, Ann. Geophys., 24, 2645–2665, 2006, http://www.ann-geophys.net/24/2645/2006/.

Burchill, J., Knudsen, D., Bock, B., Pfaff, R., Wallis, D., Clemmons, J., Bounds, S., and Stenbaek-Nielsen, H.: Core ion interactions with BB ELF, lower hybrid, and Alfven waves in the high-latitude topside ionosphere, J. Geophys. Res.-Space Phys., 109, A01219, doi:{10.1029/2003JA010073}, 2004.

Chiu, M., Von-Mehlem, U., Willey, C., Betenbaugh, T., Maynard, J., Krein, J., Conde, R., Gray, W., Hunt, J., Mosher, L., McCullough, M., Panneton, P., Staiger, J., and Rodberg, E.: ACE spacecraft, Space Sci. Rev., 86, 257–284, 1998.

Credland, J. and Schmidt, R.: The resurrection of the cluster scientific mission, ESA Bulletin-European Space Agency, pp. 5–10, 1997.

Credland, J., Mecke, G., and Ellwood, J.: The Cluster mission: ESA's spacefleet to the magnetosphere, Space Sci. Rev., 79, 33–64, 1997.

Escoubet, C. P., Berchem, J., Bosqued, J. M., Trattner, K. J., Taylor, M. G. G. T., Pitout, F., Vallat, C., Laakso, H., Masson, A., Dunlop, M., Reme, H., Dandouras, I., and Fazakerley, A.: Two sources of magnetosheath ions observed by Cluster in the mid-altitude polar cusp, Adv. Space Res., 41, 1528–1536, doi:{10.1016/j.asr.2007.04.031}, 2008.

Golovchanskaya, I. V., Ostapenko, A. A., and Kozelov, B. V.: Relationship between the high-latitude electric and magnetic turbulence and the Birkeland field-aligned currents, J. Geophys. Res.-Space Phys., 111, doi:{10.1029/2006JA011835}, 2006.

Grison, B., Sahraoui, F., Lavraud, B., Chust, T., Cornilleau-Wehrlin, N., Rème, H., Balogh, A., and André, M.: Wave particle interactions in the high-altitude polar cusp: a Cluster case study, Ann. Geophys., 23, 3699–3713, 2005, http://www.ann-geophys.net/23/3699/2005/.

Gurnett, D. and Frank, L.: Region of intense plasma-wave turbulence on auroral field lines, J. Geophys. Res.-Space Phys., 82, 1031–1050, 1977.

Gurnett, D., Huff, R., Menietti, J., Burch, J., Winningham, J., and Shawhan, S.: Correlated low-frequency electric and magnetic noise along the auroral field lines, J. Geophys. Res.-Space Phys., 89, 8971–8985, 1984.

Gustafsson, G., Bostrom, R., Holback, B., Holmgren, G., Lundgren, A., Stasiewicz, K., Ahlen, L., Mozer, F., Pankow, D., Harvey, P., Berg, P., Ulrich, R., Pedersen, A., Schmidt, R., Butler, A., Fransen, A., Klinge, D., Thomsen, M., Falthammar, C., Lindqvist, P., Christenson, S., Holtet, J., Lybekk, B., Sten, T., Tanskanen, P., Lappalainen, K., and Wygant, J.: The electric field and wave experiment for the Cluster mission, Space Sci. Rev., 79, 137–156, 1997.

Hamrin, M., Norqvist, P., Hellstrm, T., Andr, M., and Eriksson, A. I.: A statistical study of ion energization at 1700 km in the auroral region, Ann. Geophys., 20, 1943–1958, 2002, http://www.ann-geophys.net/20/1943/2002/.

Ivchenko, N. and Marklund, G.: Observation of low frequency electromagnetic activity at 1000 km altitude, Ann. Geophys., 19, 643–648, 2001, http://www.ann-geophys.net/19/643/2001/.

Johnstone, A., Alsop, C., Burge, S., Carter, P., Coates, A., Coker, A., Fazakerley, A., Grande, M., Gowen, R., Gurgiolo, C., Hancock, B., Narheim, B., Preece, A., Sheather, P., Winningham, J., and Woodliffe, R.: Peace: A plasma electron and current experiment, Space Sci. Rev., 79, 351–398, 1997.

Kasahara, Y., Hosoda, T., Mukai, T., Watanabe, S., Kimura, I., Kojima, H., and Niitsu, R.: ELF/VLF waves correlated with transversely accelerated ions in the auroral region observed by Akebono, J. Geophys. Res.-Space Phys., 106, 21123–21136, 2001.

Kintner, P., Bonnell, J., Arnoldy, R., Lynch, K., Pollock, C., and Moore, T.: SCIFER – Transverse ion acceleration and plasma waves, Geophys. Res. Lett., 23, 1873–1876, 1996.

Kintner, P., Franz, J., Schuck, P., and Klatt, E.: Interferometric coherency determination of wavelength or what are broadband ELF waves?, J. Geophys. Res.-Space Phys., 105, 21237–21250, 2000.

Knudsen, D., Clemmons, J., and Wahlund, J.: Correlation between core ion energization, suprathermal electron bursts, and broadband ELF plasma waves, J. Geophys. Res.-Space Phys., 103, 4171–4186, 1998.

Lockwood, M.: Relationship of dayside auroral precipitations to the open-closed separatrix and the pattern of convective flow, J. Geophys. Res.-Space Phys., 102, 17475–17487, 1997.

Lund, E., Mobius, E., Carlson, C., Ergun, R., Kistler, L., Klecker, B., Klumpar, D., McFadden, J., Popecki, M., Strangeway, R., and Tung, Y.: Transverse ion acceleration mechanisms in the aurora at solar minimum: occurrence distributions, J. Atmos. Solar-Terr. Phys., 62, 467–475, 2000.

Lynch, K., Bonnell, J., Carlson, C., and Peria, W.: Return current region aurora: E-parallel to, j(z), particle energization, and broadband ELF wave activity, J. Geophys. Res.-Space Phys., 107, 1115, doi:{10.1029/2001JA900134}, 2002.

Marklund, G., Blomberg, L., Falthammar, C., Erlandson, R., and Potemra, T.: Signatures of the high-altitude polar cusp and dayside auroral regions as seen by the viking electric-field experiment, J. Geophys. Res.-Space Phys., 95, 5767–5780, 1990.

Markovskii, S. A., Vasquez, B. J., and Smith, C. W.: Statistical analysis of the high-frequency spectral break of the solar wind turbulence at 1 AU, Astrophys. J., 675, 1576–1583, 2008.

Matsuoka, A., Mukai, T., Hayakawa, H., Kohno, Y., Tsuruda, K., Nishida, A., Okada, T., Kaya, N., and Fukunishi, H.: EXOS-D observations of electric-field fluctuations and charged-particle precipitation in the polar cusp, Geophys. Res. Lett., 18, 305–308, 1991.

Matsuoka, A., Tsuruda, K., Hayakawa, H., Mukai, T., Nishida, A., Okada, T., Kaya, N., and Fukunishi, H.: Electric-field fluctuations and charged-particle precipitation in the cusp, J. Geophys. Res.-Space Phys., 98, 11225–11234, 1993.

Maynard, N., Heppner, J., and Egeland, A.: Intense, variable electric-fields at ionospheric altitudes in the high-latitude regions as observed by DE-2, Geophys. Res. Lett., 9, 981–984, 1982.

Miyake, W., Matsuoka, A., and Hirano, Y.: A statistical survey of low-frequency electric field fluctuations around the dayside cusp/cleft region, J. Geophys. Res.-Space Phys., 108, 1008, doi:{10.1029/2002JA009265}, 2003.

Moen, J., Evans, D., Carlson, H., and Lockwood, M.: Dayside moving auroral transients related to LLBL dynamics, Geophys. Res. Lett., 23, 3247–3250, 1996.

Moen, J., Lockwood, M., Oksavik, K., Carlson, H. C., Denig, W. F., van Eyken, A. P., and McCrea, I. W.: The dynamics and relationships of precipitation, temperature and convection boundaries in the dayside auroral ionosphere, Ann. Geophys., 22, 1973–1987, 2004, http://www.ann-geophys.net/22/1973/2004/.

Nykyri, K., Grison, B., Cargill, P. J., Lavraud, B., Lucek, E., Dandouras, I., Balogh, A., Cornilleau-Wehrlin, N., and Rème, H.: Origin of the turbulent spectra in the high-altitude cusp: Cluster spacecraft observations, Ann. Geophys., 24, 1057–1075, 2006, http://www.ann-geophys.net/24/1057/2006/.

Onsager, T. and Lockwood, M.: High-latitude particle precipitation and its relationship to magnetospheric source regions, Space Sci. Rev., 80, 77–107, ISSI Workshop on Transport Across the Boundaries of the Magnetosphere, Bern, Switzerland, 1–5 October 1996, 1997.

Reme, H., Bosqued, J., Sauvaud, J., Cros, A., Dandouras, J., Aoustin, C., Bouyssou, J., Camus, T., Cuvilo, J., Martz, C., Medale, J., Perrier, H., Romefort, D., Rouzaud, J., dUston, C., Mobius, E., Crocker, K., Granoff, M., Kistler, L., Popecki, M., Hovestadt, D., Klecker, B., Paschmann, G., Scholer, M., Carlson, C., Curtis, D., Lin, R., McFadden, J., Formisano, V., Amata, E., BavassanoCattaneo, M., Baldetti, P., Belluci, G., Bruno, R., Chionchio, G., DiLellis, A., Shelley, E., Ghielmetti, A., Lennartsson, W., Korth, A., Rosenbauer, H., Lundin, R., Olsen, S., Parks, G., McCarthy, M., and Balsiger, H.: The Cluster ion spectrometry (CIS) experiment, Space Sci. Rev., 79, 303–350, 1997.

Sandholt, P., Denig, W., Farrugia, C., Lybekk, B., and Trondsen, E.: Auroral structure at the cusp equatorward boundary: Relationship with the electron edge of low-latitude boundary layer precipitation, J. Geophys. Res.-Space Phys., 107, 1235, doi:{10.1029/2001JA0005081}, 2002.

Schekochihin, A. A., Cowley, S. C., Dorland, W., Hammett, G. W., Howes, G. G., Quataert, E., and Tatsuno, T.: Astrophysical gyrokinetics: Kinetic and fluid turbulent cascades in magnetized weakly collisional plasmas, Astrophysical journal supplement series, 182, 310–377, doi:{10.1088/0067-0049/182/1/310}, 2009.

Shaikh, D. and Zank, G. P.: Spectral features of solar wind turbulent plasma, Monthly notices of the royal astronomical society, 400, 1881–1891, doi:{10.1111/j.1365-2966.2009.15579.x}, 2009.

Smith, C., L'Heureux, J., Ness, N., Acuna, M., Burlaga, L., and Scheifele, J.: The ACE magnetic fields experiment, Space Sci. Rev., 86, 613–632, 1998.

Stasiewicz, K., Lundin, R., and Marklund, G.: Stochastic ion heating by orbit chaotization on electrostatic waves and nonlinear structures, PHYSICA SCRIPTA, T84, 60–63, International Topical Conference on Plasma Physics – New Frontiers in Nonlinear Sciences, Faro, Portugal, 6–10 September 1999, 2000.

Sugiura, M., Maynard, N., Farthing, W., Heppner, J., Ledley, B., and Cahill, L.: Initial results on the correlation between the magnetic and electric-fields observed from the de-2 satellite in the field-aligned current regions, Geophys. Res. Lett., 9, 985–988, 1982.

Sundkvist, D., Vaivads, A., André, M., Wahlund, J.-E., Hobara, Y., Joko, S., Krasnoselskikh, V. V., Bogdanova, Y. V., Buchert, S. C., Cornilleau-Wehrlin, N., Fazakerley, A., Hall, J.-O., Rème, H., and Stenberg, G.: Multi-spacecraft determination of wave characteristics near the proton gyrofrequency in high-altitude cusp, Ann. Geophys., 23, 983–995, 2005, http://www.ann-geophys.net/23/983/2005/.

Tam, S., Chang, T., Kintner, P., and Klatt, E.: Intermittency analyses on the SIERRA measurements of the electric field fluctuations in the auroral zone, Geophys. Res. Lett., 32, L05109, doi:{10.1029/2004GL021445}, 2005.

Topliss, S., Johnstone, A., Coates, A., Peterson, W., Kletzing, C., and Russell, C.: Charge neutrality and ion conic distributions at the equatorward electron edge of the midaltitude cusp, J. Geophys. Res.-Space Phys., 106, 21095–21108, 2001.

Wahlund, J., Eriksson, A., Holback, B., Boehm, M., Bonnell, J., Kintner, P., Seyler, C., Clemmons, J., Eliasson, L., Knudsen, D., Norqvist, P., and Zanetti, L.: Broadband ELF plasma emission during auroral energization 1. Slow ion acoustic waves, J. Geophys. Res.-Space Phys., 103, 4343–4375, 1998.

Wilken, B., Axford, W., Daglis, I., Daly, P., Guttler, W., Ip, W., Korth, A., Kremser, G., Livi, S., Vasyliunas, V., Woch, J., Baker, D., Belian, R., Blake, J., Fennell, J., Lyons, L., Borg, H., Fritz, T., Gliem, F., Rathje, R., Grande, M., Hall, D., Kecsuemety, K., McKennaLawlor, S., Mursula, K., Tanskanen, P., Pu, Z., Sandahl, I., Sarris, E., Scholer, M., Schulz, M., Sorass, F., and Ullaland, S.: RAPID - The imaging energetic particle spectrometer on Cluster, Space Sci. Rev., 79, 399–473, 1997.